

## Full Length Article

# Experimental investigation of poultry litter gasification and co-gasification with beech wood in a bubbling fluidised bed reactor – Effect of equivalence ratio on process performance and tar evolution



Giannis Katsaros<sup>a,\*</sup>, Daya Shankar Pandey<sup>a,b,\*</sup>, Alen Horvat<sup>c</sup>, Guadalupe Aranda Almansa<sup>e</sup>, Lydia E. Fryda<sup>e</sup>, James J. Leahy<sup>d</sup>, Savvas A. Tassou<sup>a</sup>

<sup>a</sup> RCUK Centre for Sustainable Energy Use in Food Chains (CSEF), Brunel University London, Uxbridge UB8 3PH, UK

<sup>b</sup> School of Engineering and the Built Environment, Anglia Ruskin University, Chelmsford CM1 1SQ, UK

<sup>c</sup> Carlos III University of Madrid, Energy Systems Engineering Group, Thermal and Fluids Engineering Department, Avda. de la Universidad 30, 28911 Leganés, Madrid, Spain

<sup>d</sup> Carbolea Research Group, Department of Chemical Sciences, Bernal Institute, University of Limerick, Limerick V94 T9PX, Ireland

<sup>e</sup> Energy Research Centre of the Netherlands, Biomass and Energy Efficiency, Petten, The Netherlands

## ARTICLE INFO

## Keywords:

Poultry litter  
Gasification  
Tar  
Agglomeration  
Beech wood  
Equivalence ratio

## ABSTRACT

The effect of equivalence ratio on gasification of poultry litter, blend of poultry litter with beech wood and beech wood alone, was experimentally studied in a lab-scale fluidised bed reactor. Lower calorific value decreased with equivalence ratio whereas carbon conversion efficiency revealed the opposite trend. Beech wood showed both the highest lower calorific value and carbon conversion efficiency, 4.96 MJ/m<sup>3</sup> and 91.6% respectively. Total gas chromatography-detectable tar decreased with an increase in equivalence ratio. The reduction in total gas chromatography-detectable tar was more profound in the case of poultry litter (22%). Beech wood illustrated the highest amount of total gas chromatography-detectable tar, 7.52g<sub>tar</sub>/kg<sub>feedstock-daf</sub> at the lowest equivalence ratio, due to the higher lignin content responsible for generation of polycyclic aromatic hydrocarbons. Agglomeration occurred while gasifying poultry litter at 750 °C and at the highest equivalence ratio (0.25), whereas in the case of blend and beech wood alone all the test runs were conducted successfully.

## 1. Introduction

The depletion of fossil fuels along with the associated emission of greenhouse gases in the atmosphere makes urgent the need for exploration of renewable energy resources [1]. Among those resources, bioenergy has recently gained a lot of attention. According to Bioenergy Europe [2], bioenergy accounts for 63% of the renewable energy share within the EU28. Reasons explaining these trends are the vast production potential and its environmentally friendly nature. In particular, significant amounts of biomass can be derived from woody residues (parks, residues from managed forests, wood industry), agricultural including animal waste, and solid fraction of municipal waste [3]. When using residual streams, the feedstock is considered ideally CO<sub>2</sub> neutral, since it is produced through photosynthesis process during which the amount of CO<sub>2</sub> that is absorbed from the atmosphere is

exactly the same to the amount released by biomass use [4]. However, there is always some net addition of CO<sub>2</sub> in the atmosphere due to the utilisation of fertilisers and fossil fuels during the phases of production and handling and transportation of biomass.

Poultry litter (PL) is a blend of poultry excreta, animal feed, bedding material (straw, sand or wood chips) and feathers. Due to the growing demand for poultry meat globally, PL has become a major source of waste from poultry industry and its effective disposal is a major challenge for farm owners. Therefore, the traditional landfilling is not anymore a sustainable and economically viable option [5], whereas the common practise of utilising PL as a fertiliser poses significant environmental issues due to high concentration of PL in confined areas. Particularly, excessive amounts of PL spread into soil can lead to eutrophication, nitrate leaching, crop toxicity, odours and emissions of greenhouse gases (NH<sub>3</sub>, NO<sub>x</sub>, N<sub>2</sub>O) to the atmosphere [6–8].

*Abbreviations:* BW, Beech Wood; CGE, Cold Gas Efficiency; CCE, Carbon Conversion Efficiency; ECN, The Energy Research Centre of the Netherlands; ER, Equivalence Ratio; FID, Flame Ionisation Detector; GC, Gas Chromatography; g, grams; LCV, Lower Calorific Value; PAH, Polycyclic Aromatic Hydrocarbons; PL, Poultry Litter; PL/BW, Poultry Litter with Beech Wood; SPA, Solid Phase Adsorption

\* Corresponding authors at: RCUK Centre for Sustainable Energy Use in Food Chains (CSEF), Brunel University London, Uxbridge UB8 3PH, UK (D.S. Pandey).

E-mail addresses: [ioannis.katsaros@brunel.ac.uk](mailto:ioannis.katsaros@brunel.ac.uk) (G. Katsaros), [daya.pandey@anglia.ac.uk](mailto:daya.pandey@anglia.ac.uk) (D.S. Pandey).

<https://doi.org/10.1016/j.fuel.2019.116660>

Received 22 July 2019; Received in revised form 19 October 2019; Accepted 12 November 2019

Available online 18 November 2019

0016-2361/ Crown Copyright © 2019 Published by Elsevier Ltd. This is an open access article under the CC BY license

(<http://creativecommons.org/licenses/by/4.0/>).

Increased environmental concerns described above and strict regulations pertaining to the use of PL in fertiliser applications necessitate the implementation of alternative strategies regarding PL management. In this context, thermochemical conversion of PL into energy can be a viable option. Produced energy can be used onsite, saving the farm owners from significant fossil fuel costs, while mitigating the environmental effects resulting from the utilisation of conventional fuels and the over application of PL as a fertiliser.

The thermochemical conversion pathways are categorised into combustion, pyrolysis and gasification. The former is already proven and commercialised, whereas gasification and pyrolysis have to overcome specific challenges before they can be further employed at full commercial scale, particularly when using manure-based feedstock. Focusing on gasification technology, a carbon-based feedstock is dissociated in a high temperature environment (700–1500 °C) under sub-stoichiometric conditions. The oxidising medium can be air, steam, pure oxygen or a mixture of them. The product of gasification is a combustible gas, known as the “product gas” or “syngas”, consisting mainly of CO, H<sub>2</sub>, CO<sub>2</sub>, CH<sub>4</sub> and a small amount of C<sub>2</sub>+ compounds along with impurities, such as fine particulates, tar and alkali metals [9]. Gasification is considered as a more flexible technology compared to combustion since the product gas can be utilised in a wide range of applications, being that heat and power generation, biofuel production and chemicals [10]. However, the major problem impeding its further development is the presence of tar in the product gas. Different definitions of tar exist across the literature, with one of the most common describing tar as “the organics produced under thermal or partial-oxidation regimes (gasification) of any organic material, and are generally assumed to be largely aromatic” [11]. The main issue from the presence of tar relates to their condensation in the colder sections of the gasifier which further results in clogging and fouling of the equipment downstream. A comprehensive review of the nature and tar formation is presented by Milne *et al.* [12]. The authors classified tar into primary, secondary and tertiary, based on their formation at different process conditions. Primary tar is mostly oxygenated compounds such as levoglucosan, glycolaldehyde and furfural that are formed during the pyrolysis stage at temperatures between 400 and 600 °C. As the temperature increases, primary tar compounds decompose and convert into secondary tar, mostly consisting of phenolics and olefins at temperatures between 700 and 850 °C. At even higher temperatures (850–1000 °C) tertiary tar is formed, consisting complex poly-aromatic hydrocarbons (PAH) and these are very stable with a high dew point [13–15].

PL is considered a fuel of low energetic value due to the high moisture and ash content. Furthermore, PL ash comprises of inorganic materials (K, P, Mg, Si) characterised by low melting temperature which may lead to agglomeration conditions and consequently defluidisation of the gasifier bed. Due to the specific challenges outlined above, co-gasification of poultry litter with traditional biomass can be an attractive option. A number of researchers have conducted work on poultry litter gasification [16–22]. However, the possibility of co-gasification of PL with biomass has been rarely explored. Experiments were conducted with a mixture of 70% wood chips and 30% PL in a 10 kW fixed bed downdraft gasifier [23]. The authors argued that the product gas was of comparable quality with the one of gasification of pure wood, implying the suitability of PL as feedstock in gasification processes. In another study, experiments were performed on a lab-scale fixed bed gasifier of 5 kg/h feeding rate [24]. Pre-dried raw PL and pelletised PL were mixed with wood pellets in order to study the properties of product gas generated by the two different blends. The study recommended that co-gasification of PL with wood is technically feasible, and the product gas from pelletised PL has a higher calorific value compared to that of raw PL.

The objective of the present study is to evaluate the effect of equivalence ratio (ER) on gasification performance of PL, the blend of PL with beech wood (PL/BW) at 50 – 50% mass ratio and pure BW in a

**Table 1**  
Ultimate and proximate analysis of feedstock.

Type of feedstock	PL	PL/BW	BW
<i>Proximate analysis (% w/w, a.r.)</i>			
Moisture	9.71	9.94	9.00
Volatile matter	69.60	73.90	80.90
Ash	14.30	8.10	1.30
Fixed carbon*	16.10	17.90	17.80
<i>Ultimate analysis (% w/w, d.b.)</i>			
C	42.82	46.76	46.85
H	5.49	5.68	6.30
N	3.90	2.48	0.17
Cl	0.25	0.16	0.01
S	0.60	0.37	0.02
O*	32.64	36.45	45.35
LCV (MJ/kg d.b)	16.78	17.37	17.59

a.r.: as received, d.b.: dry basis, \*calculated by difference.

lab-scale bubbling fluidised bed reactor. The key outcome of the study is that it highlights the operating temperature limitations when using poultry litter in gasification. Furthermore, this study also provides detailed practical insight about the differences in total tar amount and the chemical composition of evolved tar from the three tested fuels, which to the best of authors' knowledge are not well reported in the literature.

## 2. Experimental investigation

### 2.1. Materials

PL was collected from a poultry farm in Finland. Due to its heterogeneous nature, PL was partially dried and sieved at a particle size between 0.5 and 0.98 mm before being fed into the gasifier. Beech wood, originally from Germany [25] was provided by ECN part of TNO in which the experiments took place. This woody stream is mainly used for bedding material in animal keeping. The particle size of BW was in the range of 0.7–2 mm. The moisture content in the feedstocks was measured on as received (a.r.) basis. The PL and BW were blended at 50–50% (by weight) before co-gasification experiments. Table 1 reports ultimate and proximate analysis and the lower calorific value (LCV) of all the fuels used in this study. The value of fixed carbon was calculated by subtracting the percentages of volatile matter and ash from 100% on a dry basis (d.b.). Similarly, the oxygen content was determined by the difference from the elements presented in ultimate analysis and the ash content.

The chemical composition of ash measured with inductive coupled plasma technology is presented in Table 2. It is evident that the concentration of silicon, potassium, phosphorus and calcium in the PL ash is significantly higher compared to the blend of PL and BW. This relates to the agglomeration phenomenon and is discussed in Section 3.4.

### 2.2. Experimental facility

The experimental set up illustrated in Fig. 1 is located at the Energy Research Centre of the Netherlands, now part of the Netherlands organisation of applied research TNO (ECN part of TNO). The experiments were conducted in the framework of the EU's BRISK2 Transnational Access Project. The fuel was fed into the reactor by two mechanical screw feeders under a limited flow of nitrogen (1.0 L/min) in order to avoid any backflow of the product gases. The hopper was equipped with a stirrer to avoid bridging and maintain consistent flow of the feedstock. The reactor consists of two different zones: a bed section with an internal diameter of 74 mm and 500 mm height with a perforated distribution plate at its base, and the freeboard section with an internal diameter of 108 mm and height 600 mm. The fluidising medium (air and nitrogen) is electrically heated to 160 °C prior to introduction from the bottom of the reactor through the perforated

**Table 2**  
Chemical composition of ash.

Ash composition (mg/kg d.b.)	PL	PL/BW	BW
<i>Major components</i>			
Aluminium	1200	336	65
Calcium	15500	8947	2964
Iron	1600	868	99
Magnesium	8200	4299	503
Sodium	4200	1661	36
Phosphorus	10200	5603	104
Potassium	27700	12866	1331
Silicon	7300	147	242
Titanium	95	87.50	4
<i>Minor components</i>			
Arsenic	< 0.5	1.03	n.d.
Cadmium	0.14	< 0.25	n.d.
Cobalt	1.9	2.28	n.d.
Chromium	16	40.70	2
Copper	84	89.80	3
Mercury	< 0.02	0.04	n.d.
Manganese	600	346	94
Molybdenum	4.80	7.03	n.d.
Nickel	16	37.20	2
Lead	1.50	1.87	n.d.
Antimony	< 0.5	< 0.25	n.d.
Vanadium	4.20	4.29	n.d.
Zinc	450	238	3

n.d.: not detected.

distribution plate. Gas exiting the freeboard section passes through a solid-gas separator (cyclone) in order to remove entrained particles of char and ash. After the cyclone, product gas splits into two streams: one heading towards a flare where it is combusted and a second one passing through two filters in order to remove the tar and finest particles that were not captured from the cyclone. Clean gas exiting the filters passes through an on-line gas analyser where its composition is continuously monitored. Tar and moisture samples are collected through a sampling port located between the hot and the cold filter. It is worth mentioning that the temperature in the sections from the exit of the reactor up to the cold filter is maintained at 400 °C, preventing any tar condensation inside the pipes. This is realised through insulation and electric heating.

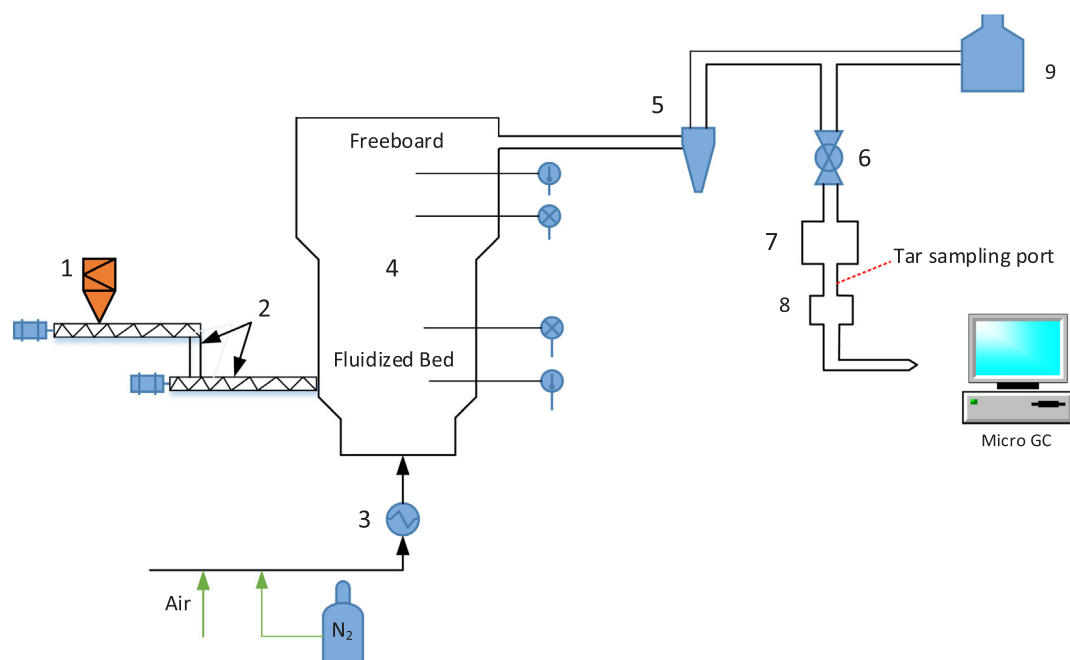


**Fig. 1.** Lab-scale experimental facility at ECN part of TNO, Netherlands 1: Hopper, 2: Screw feeders, 3: Pre-heater, 4: Gasifier, 5: Cyclone, 6: Valve, 7: Hot filter, 8: Cold filter, 9: Flare.

### 2.3. Test procedure

Three tests were conducted on each day and the fuel feeding rate reported is the average of the utilised fuel in each test. The start-up period for all experiments was between 1.5 and 2 h, during which the reactor was heated by means of electrical heating. Air and nitrogen were continuously supplied from the bottom at a constant flow rate of 12.0 L/min in order to keep adequate fluidisation and to ensure consistent time for gasification conditions (residence time). Experiments were carried out at different ERs by adjusting the flow rate of air and nitrogen entering the reactor. More specifically, at lower ER the flow rate of air was reduced while the nitrogen was increased and vice versa, while maintaining the total flow rate at 12 L/min. During all the experiments the temperature of the reactor was kept constant at 750 °C. Sieved silica sand (1.06 kg/day) with a particle size of 0.25–0.5 mm was used as a bed material. Wen and Yu's correlation was used [26] to calculate the minimum theoretical fluidisation velocity at the specified operating conditions which was 0.033 m/s. A summary of the experimental tests is presented in Table 3. Only two tests regarding PL gasification are reported (test 1, 2) since agglomeration occurred at the highest ER (0.25). Tests 3, 4, 5 refer to PL/BW gasification. An attempt was made to gasify the PL/BW at the temperature of 800 °C but the bed agglomerated and the experiment was terminated. BW alone was gasified at 750 °C (tests 6, 7, 8) and the results are considered as the reference point. It can be seen from Table 3 that the feeding rate was consistent throughout the experimental campaign.

### 2.4. Measurement methods

An ABB gas analyser (CO, CO<sub>2</sub>, CH<sub>4</sub>, H<sub>2</sub>, O<sub>2</sub>) and a Varian micro-GC analyser (Ar/O<sub>2</sub>, CO, CO<sub>2</sub>, CH<sub>4</sub>, C<sub>2</sub>H<sub>2</sub>, C<sub>2</sub>H<sub>4</sub>, C<sub>2</sub>H<sub>6</sub>, C<sub>6</sub>H<sub>6</sub>, C<sub>7</sub>H<sub>8</sub>, H<sub>2</sub>S, and COS) were used for the on-line measurement of the product gas compositions. The measurements took place continuously at 4-minute intervals. Neon (10 mL/min) was added as tracer gas to measure the flowrate of the product gas and was used to calculate the mass balances. Samples of elutriated char and ash from both the cyclone and bed material were taken and further analysed for the mass balance calculations. In the case of cyclone, the material was collected at the end of each test, whereas the bed material samples were collected at the end of

**Table 3**  
Summary of operating conditions of experimental tests.

Type of feedstock	PL		PL/BW			BW		
	1	2	3	4	5	6	7	8
Fuel flow rate (kg/hour, a.r.)	0.548	0.548	0.559	0.559	0.559	0.546	0.546	0.546
ER (-)	0.17	0.21	0.17	0.21	0.25	0.18	0.225	0.27
Air flow rate (litres/min)	6.05	7.6	6.5	8.2	9.8	6.05	7.6	9.08
Nitrogen flow rate (litres/min)	5.95	4.4	5.5	3.8	2.2	5.95	4.4	2.92
Minimum fluidisation velocity $U_{mf}$ (m/sec)	0.033	0.033	0.033	0.033	0.033	0.033	0.033	0.033
Superficial fluidisation velocity $U$ (m/sec)	0.138	0.138	0.138	0.138	0.138	0.138	0.138	0.138
Gasifier temperature ( $^{\circ}$ C)	750	750	750	750	750	750	750	750
Fluidisation medium temperature ( $^{\circ}$ C)	160	160	160	160	160	160	160	160

**Table 4**  
Summary of results derived from all the experimental tests at steady state conditions.

Test Number	1	2	3	4	5	6	7	8
H <sub>2</sub> (vol.%, d.b.)	10.1	10.15	6.54	7.97	6.63	6.45	7.15	6.31
N <sub>2</sub> (vol.%, d.b.)	64.4	62.8	65.54	63.42	63.18	63.7	61.48	59.96
CH <sub>4</sub> (vol.%, d.b.)	2.2	2.12	3.42	3.21	3.14	3.79	3.73	3.78
CO (vol.%, d.b.)	11.18	11.39	11	10.65	10.59	12.74	12.82	13.52
CO <sub>2</sub> (vol.%, d.b.)	10.21	11.59	11.29	12.59	14.21	11.1	12.65	14.21
C <sub>2</sub> H <sub>4</sub> (vol.%, d.b.)	1.17	1.13	1.34	1.24	1.24	1.25	1.21	1.24
C <sub>2</sub> H <sub>6</sub> (vol.%, d.b.)	0.198	0.2	0.2	0.2	0.2	0.18	0.19	0.19
C <sub>2</sub> H <sub>2</sub> (vol.%, d.b.)	0.02	0.02	0.05	0.04	0.04	0.05	0.05	0.05
H <sub>2</sub> S (ppmv, d.b.)	365.7	369	272.56	243.15	198.45	24	28.6	31.6
COS (ppmv, d.b.)	17	18.86	17.28	17.46	15.36	< 3	< 3	< 3
C <sub>6</sub> H <sub>6</sub> (ppmv, d.b.)	384.5	393.8	876.3	835	866	1945	1289.9	967.9
C <sub>7</sub> H <sub>8</sub> (ppmv, d.b.)	176.6	181.5	341.72	340.83	321.98	735	455	265.23
Total GC-detectable tar (gtar/kg <sub>feedstock-daf</sub> )	4.87	4.25	6.46	6.1	5.8	7.52	7.44	6.72
Gas yield (Nm <sup>3</sup> dry N <sub>2</sub> free/kg <sub>feedstock-daf</sub> )	1.221	1.247	0.972	0.983	0.97	0.86	0.948	0.976
Moisture (g/Nm <sup>3</sup> dry product gas)	64.5	67	100	111.5	113.5	90	111.5	133
LCV (MJ/Nm <sup>3</sup> , d.b.)	4.22	4.2	4.47	4.43	4.25	4.96	4.86	4.82
CGE (%)	61	58	55	55.93	57.85	62.93	62.78	61.96
CCE (%)	85.5	85.1	76.8	78.9	84	82.76	86.63	91.6

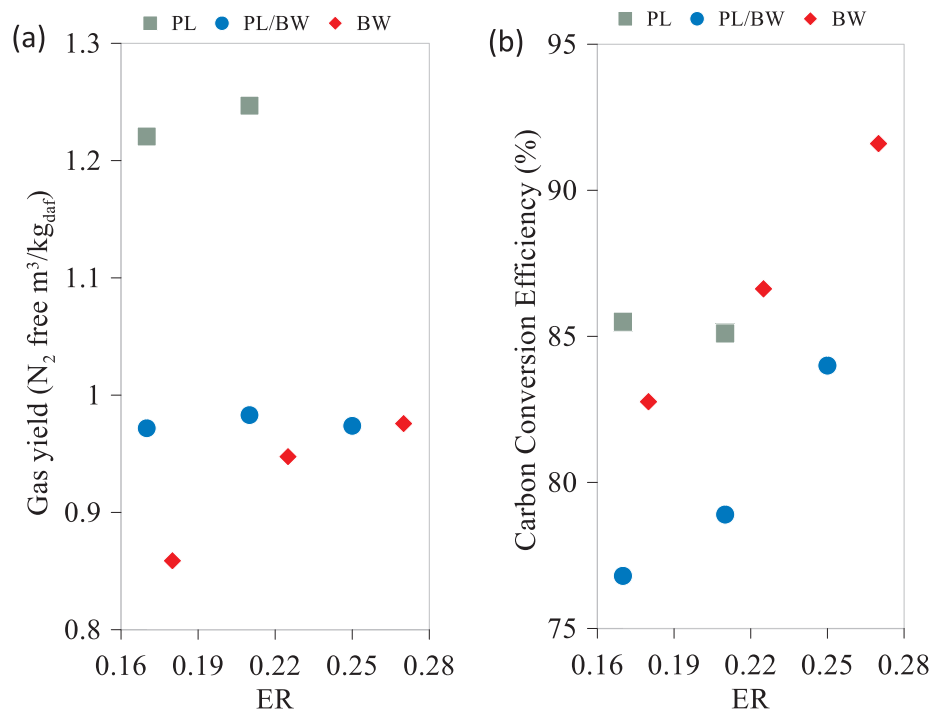


**Fig. 2.** Effect of ER on a) Gas yield and b) CCE.

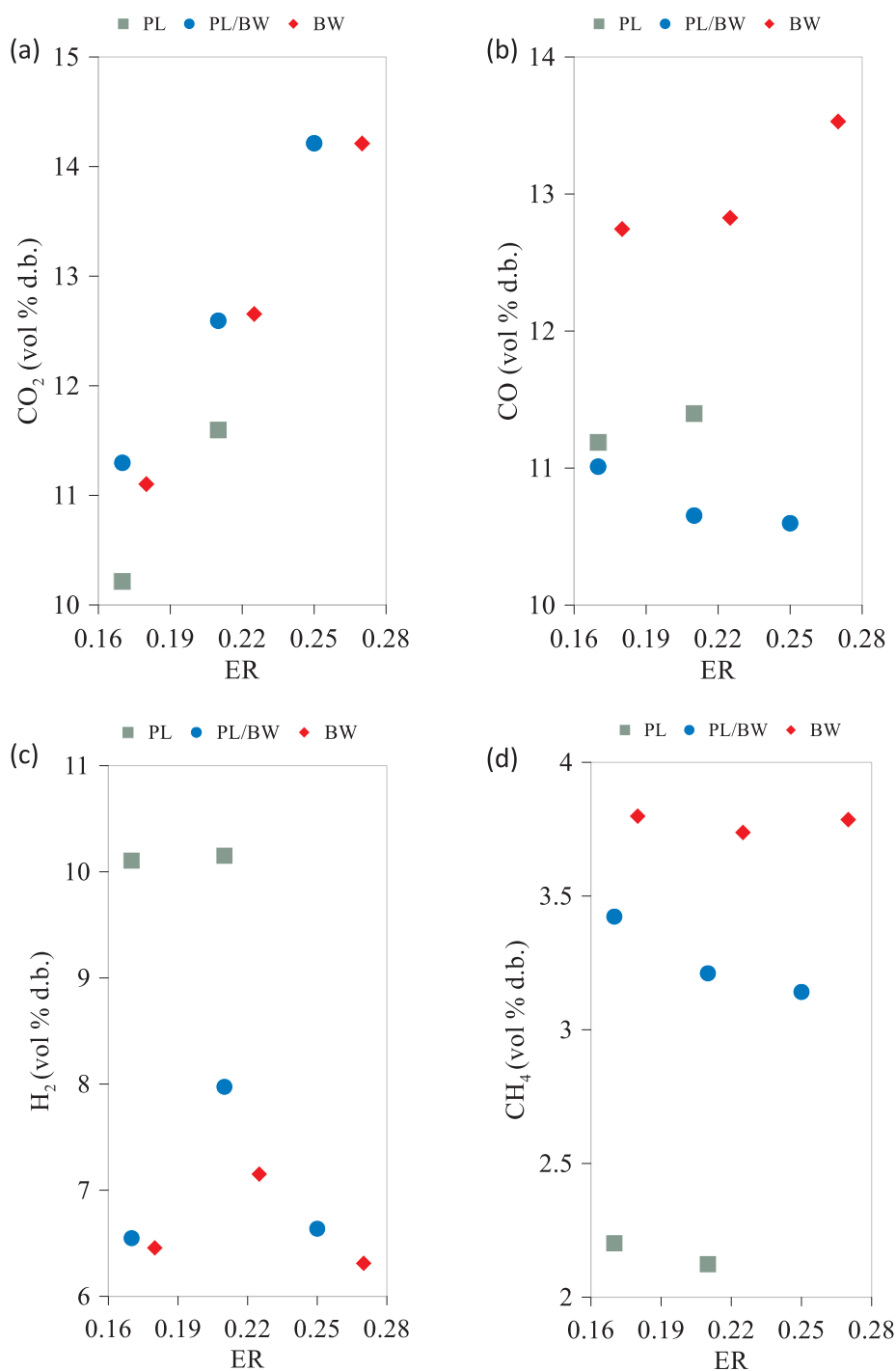


Fig. 3. Evolution of the major gas species as a function of ER.

the day.

Off-line solid phase adsorption (SPA) method was used for the analysis of tar compounds. Total GC-detectable tar reported in this study refers to the sum of tar compounds eluting from thiophene ( $M \sim 84$  g/mol) to benzo[a]anthracene ( $M \sim 228$  g/mol). Benzene ( $\text{C}_6\text{H}_6$ ) and toluene ( $\text{C}_7\text{H}_8$ ) yields were measured by on-line micro-GC and presented as permanent gases and not as tar compounds. Tar yields are reported on a mass basis in order to avoid any dilution effects due to changes in ER. Three SPA samples of 100 mL of product gas were extracted from the reactor with a syringe pump at each gasification test. The sampling period was 2 min and the temperature of the gas at the sampling port was maintained at 400 °C. The tar from the product gas

condensed and adsorbed on 500 mg of aminopropyl silica sorbent. Tar was eluted from the aminopropyl silica sorbent immediately after sampling by the addition of  $3 \times 600$  mL of dichloromethane and further analysed by gas chromatography. Two different instruments were used, an Agilent 7890A GC coupled to a mass detector (triple-axis MSD 5975C) for the identification of tar compounds and a Thermo Scientific Trace 1310 GC with flame ionisation detector (FID) for the quantification of the tar compounds. A more detailed description of the sampling and extraction processes along with the equipment used can be found elsewhere [27]. Moisture measurement was performed by placing an impinger containing 100 mL of phosphorus pentoxide ( $\text{P}_2\text{O}_5$ ), a powerful desiccant, in a water bath of 4 °C in order to trap the moisture

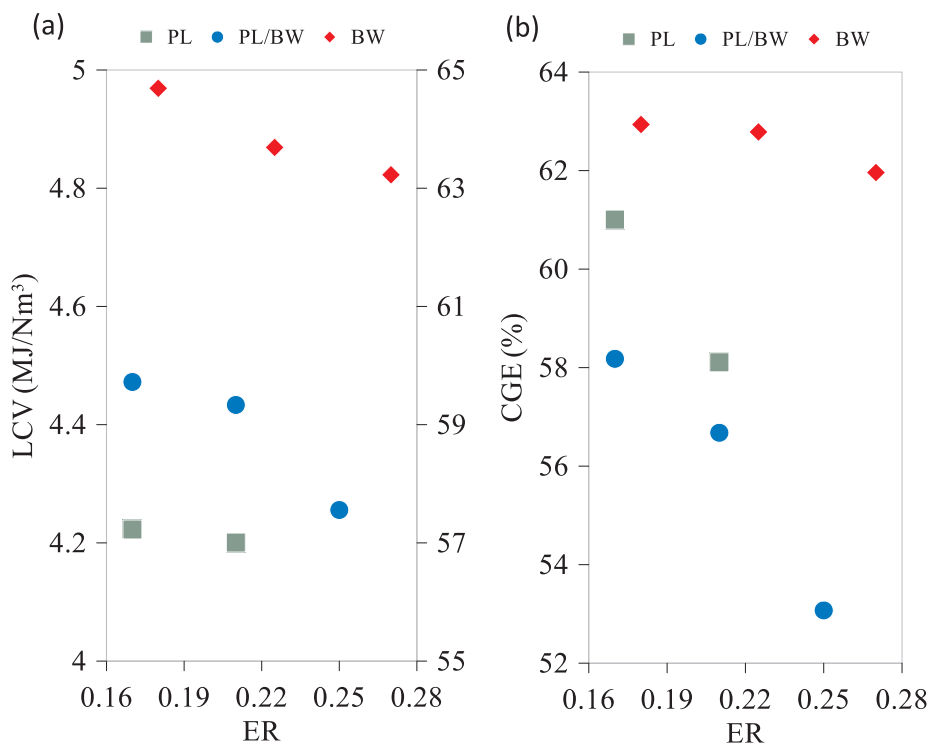


Fig. 4. Effect of ER on a) LCV and b) CGE.

into the solvent. After the completion of the gasification test, the impinger was weighted and the moisture content calculated by the mass difference between the impinger before and after the measurement [28].

### 2.5. Performance analysis

Cold gas efficiency (CGE), carbon conversion efficiency (CCE), LCV, gas and tar yields were analysed to evaluate the performance of the gasification process. It should be highlighted that all the calculations were performed on a dry basis and the tar compounds were excluded from LCV. CGE is defined as the ratio of the chemical energy of the product gas to the chemical energy contained in the initial fuel, whereas CCE is defined as the ratio between the carbon converted into gas to the carbon fed into the gasifier.

## 3. Results and discussion

Table 4 represents a summary of the main results derived during the whole experimental campaign. Results include permanent gas composition, total GC-detectable tar and moisture content in the product gas, along with process performance parameters CGE and CCE. It is important to mention that the compositions of gases presented in Table 4 are the average values of four consecutive measurements once the gasification process achieved the steady state condition.

### 3.1. Gas yield and carbon conversion efficiency (CCE)

The effect of ER on the total gas yield is shown in Fig. 2(a) and it is reported on a nitrogen and dry ash free (daf) basis ascertaining the actual gas production without any dilution effects. As observed, PL results in the highest amount of total gas yield of  $1.25 \text{ m}^3/\text{kg}_{\text{daf}}\text{N}_{2\text{free}}$  at an ER of 0.21. Moreover, with an increase in ER, the gas yield from poultry litter and BW showed an upward trend, probably due to higher char conversion and release of volatiles since more oxygen is consumed in the reactor. On the other hand, the gas yield resulted from gasification of PL/BW blend remains fairly constant at the tested ER range.

The possible explanation for the inconsistency in the gas yield during the co-gasification of blended PL/BW could be either due to high attrition and char entrainment or due to increased  $\text{N}_2$  concentration in the dry gas. Indicatively, the measured carbon content in cyclone fines and bed ash collected from PL/BW was reported to be higher (18 g/hour) compared to the BW alone (8.9 g/hour), confirming the higher carbon entrainment. CCE shown in Fig. 2(b), is increasing with ER, implying that higher amounts of char are converted due to increased amounts of oxygen available in the reactor. It should be noted that during test 2, a small fraction of bed material was extracted due to high ash accumulation in the bed which might have affected the CCE calculation resulting in the drop of CCE.

### 3.2. Gas composition

Fig. 3 presents the gas composition of the main gaseous species as a function of ER. An increase in  $\text{CO}_2$  content with ERs can be observed for all the tested fuels. This is attributed to the higher availability of oxygen in the reactions with volatiles and char combustion. The results related to  $\text{CO}_2$  concentration are in line with the findings of previous research reported in [17,29,30]. In general, the presence of oxygen in the reactor decreases the concentration of CO due to its oxidation and formation of the more stable compound  $\text{CO}_2$ . However, the concentration of CO in this study shows different behaviour with respect to the fuels. Particularly, for PL and BW it increases while the blend of PL and BW showed an opposite trend. A possible explanation could be decomposition of higher hydrocarbons resulting in an increase of the CO concentration. The tar analysis presented in Fig. 5 confirmed this by analysing the GC-detectable tar conversion over the tested range of ER. Noticeable decrease in the concentrations of  $\text{C}_6\text{H}_6$  and  $\text{C}_7\text{H}_8$  (see Table 4) can be seen in BW explaining the observed increase in CO concentration. A similar conclusion was drawn by Kwapinska *et al.* [28] from gasification of *Miscanthus × giganteus* at ER ranging between 0.18 and 0.32. Additionally, an increase in ER can affect the optimal mixing conditions and could be the possible reason for higher concentrations of CO, since local spots may be created with very low air concentrations. As a consequence of imperfect mixing higher amounts

**Table 5**  
Identified tar compounds with the chromatographic retention times.

Poultry litter (PL)		Beech wood (BW)	
Tar compound	Retention time (min)	Tar compound	Retention time (min)
1	Thiophene	2.96	//
2	Pyridine*	4.54	//
3	Pyrrrole*	5.12	//
4	Methyl pyridine*	7.24	//
5	Methyl pyrazine *	7.54	//
6	Ethylbenzene	8.69	Ethylbenzene 8.70
7	o/m/p Xylene	8.95	o/m/p Xylene 8.97
8	Phenylethyne	9.37	Phenylethyne 9.43
9	Styrene	9.74	Styrene 9.78
10	Iso-dimethyl pyridine*	10.97	//
11	Ethenyl pyridine*	11.11	//
12	Benzonitrile*	13.15	//
13	Phenol	13.95	Phenol 13.52
14	o/m/p Methyl styrene	14.66	o/m/p Methyl styrene 14.59
15	Indene	15.06	Indene 15.07
16	o/m/p Cresol	16.34	o/m/p Cresol 15.98
	Naphthalene, 1,2 dihydro	18.43	Naphthalene, 1,2 dihydro 18.38
17	Naphthalene	19.35	Naphthalene 19.37
18	Quinoline*	21.11	//
19	Isoquinoline*	21.36	//
20	Indole*	22.79	//
21	2-Methyl naphthalene	22.97	2-Methyl naphthalene 22.50
22	Biphenyl	24.86	Biphenyl 24.83
23	//		Ethenyl naphthalene 26.07
	Acenaphthylene	26.49	Acenaphthylene 26.46
24	Acenaphthene	27.40	Acenaphthene 27.37
25	Dibenzofuran	28.28	Dibenzofuran 28.24
26	Fluorene	29.77	Fluorene 29.69
27	Phenanthrene	34.04	Phenanthrene 33.97
28	Anthracene	34.36	Anthracene 34.27
29	4H-Cyclopenta(def) phenanthrene	36.67	4H-Cyclopenta(def) phenanthrene 36.59
30	2-Phenyl naphthalene	37.71	//
31	Fluoranthrene	38.96	Fluoranthrene 38.86
32	Pyrene	39.64	Pyrene 39.54
	//		Benzo[a/b]fluorene 40.89
33	Benzo[a]anthracene	43.91	Benzo[a]anthracene 43.90
34	//		Benzo(k) fluoranthrene 47.56

of unconverted fuel is expected (see section 3.1 for the case of PL/BW blend). The concentration of H<sub>2</sub>, although expected to decrease with increasing ERs due to oxidation, in the cases of BW and blend it fluctuates, while in the two test runs of PL it remains approximately stable. Similarly, the fluctuations in H<sub>2</sub> concentration could also be attributed to the decomposition of higher hydrocarbons. Methane concentration shows a relatively stable trend for all fuels which is mainly produced in the pyrolysis zone. The steam reforming of CH<sub>4</sub> is kinetically limited and unlikely to occur at temperatures below 1000 °C [29,31]. Furthermore, an increase in ER promotes the decomposition of tar compounds into lighter hydrocarbons, a fact that could explain the observed decrease in C<sub>7</sub>H<sub>8</sub> concentration in this study. Finally, the compositions of lighter hydrocarbons (C<sub>2</sub>H<sub>2</sub>, C<sub>2</sub>H<sub>4</sub>, and C<sub>2</sub>H<sub>6</sub>) seem not to be affected by changes in ER (Table 4).

### 3.3. LCV and CGE

Fig. 4(a) displays the effect of ER on the LCV of all tested fuels. In line with [17,29,32–35], the LCV of the product gas decreased with an increase in ER. The explanation stems from the fact that at higher ERs there is a higher amount of oxygen available to react with volatiles

evolving in the pyrolysis zone and further extension afterwards of oxidation reactions. In all cases the decrease in LCV is small (< 5%). This can be explained from the fluctuations in the composition of H<sub>2</sub>, CO and higher hydrocarbons. Especially higher hydrocarbons (C<sub>6</sub>H<sub>6</sub>, C<sub>7</sub>H<sub>8</sub>), although present in small quantities, they have much higher LCV compared to H<sub>2</sub> and CO and therefore even a small change can have a significant effect on LCV. BW acquires the highest LCV accounting for 4.96 MJ/Nm<sup>3</sup>, followed by PL/BW and PL respectively. The effect of ER on CGE is presented in Fig. 4(b) and shows a declining trend with ERs. At higher ER, the higher amount of air injected in the gasifier promotes carbon and hydrogen oxidation, resulting in the decrease of the chemical energy contained in the product gas. The obtained values of CGE are within the limits (50–80%) which are in line with findings given by Arena [36] for gasification of municipal solid waste with air and oxygen enriched air. Among the fuels tested in this study, BW has the highest CGE (63%).

### 3.4. Agglomeration

PL ash contains high amounts (Table 2) of inorganic compounds (P, K, Mg, Si) characterised by low melting temperatures. This can lead to agglomeration which severely affect the operational stability of the gasifier. In the specific experimental campaign, agglomeration indeed occurred in the case of PL at 750 °C and highest tested ER (0.25) causing the immediate shutdown of the gasifier. Adding beech wood fuel with very low ash content at 50–50% mass ratio helped to mitigate this effect and the gasifier was able to run successfully at 750 °C at all tested ERs. However, increasing the temperature to 800 °C resulted again in the formation of agglomerates inside the gasifier, showing the operational limit when using PL as fuel.

### 3.5. Tar analysis

Table 5 presents the identified tar compounds in the order they were eluted. The tar compounds derived from the blend of PL/BW are not shown because they are the same with the respective ones eluted for PL alone. It can be observed from Table 5 that the main difference between PL and BW are the nitrogen-containing tar compounds reflecting the high nitrogen content of PL compared to BW. Ten nitrogen-containing tar compounds were identified and reported in Table 5 (designated by \*). In addition to that sulphur-containing tar compound, thiophene was identified in PL derived tar.

Fig. 5 depicts the effect of ER on the amount of total GC-detectable tar. It is evident that there is a decrease in total GC-detectable tar for all fuels at rising ERs. The most significant decrease relates to the total GC-detectable tar of PL (21.8%) while the other two fuels present a similar decreasing rate (10.1% for PL/BW and 10.7% for BW). A possible explanation for the decrease in tar yield may be the oxidation of tar compounds due to the higher presence of oxygen within the reactor. The results are in line with previous work of Hanping *et al.* [37]. The authors gasified three different biomass samples at an ER ranging between 0.15 and 0.35 and temperature set at 800 °C, reporting a considerable reduction of tar in rising ERs. On the contrary, a more recent study carried out by Horvat *et al.* [38] found that at constant temperature, the ER has relatively little impact on the yield or composition of tar from a grassy biomass. Campoy *et al.* [29] performed gasification experiments of different feedstocks and found that the maximum decrease in the gravimetric tar content was 40% for orujillo (exhausted olive cake) when increasing the ER from 0.23 to 0.43. However, the experiments took place in a pilot scale reactor where temperature was ER dependent, thus tar evolution cannot be studied separately.

Low tar yields of PL can be attributed to its high ash content along with the low organic fraction (low lignin content) compared to BW. PL ash contains significant amounts of inorganics (Table 2) that acts as tar cracking catalysts causing a reduction in the total amount of tar [39]. Lignin was reported to be a tar precursor producing higher total GC-

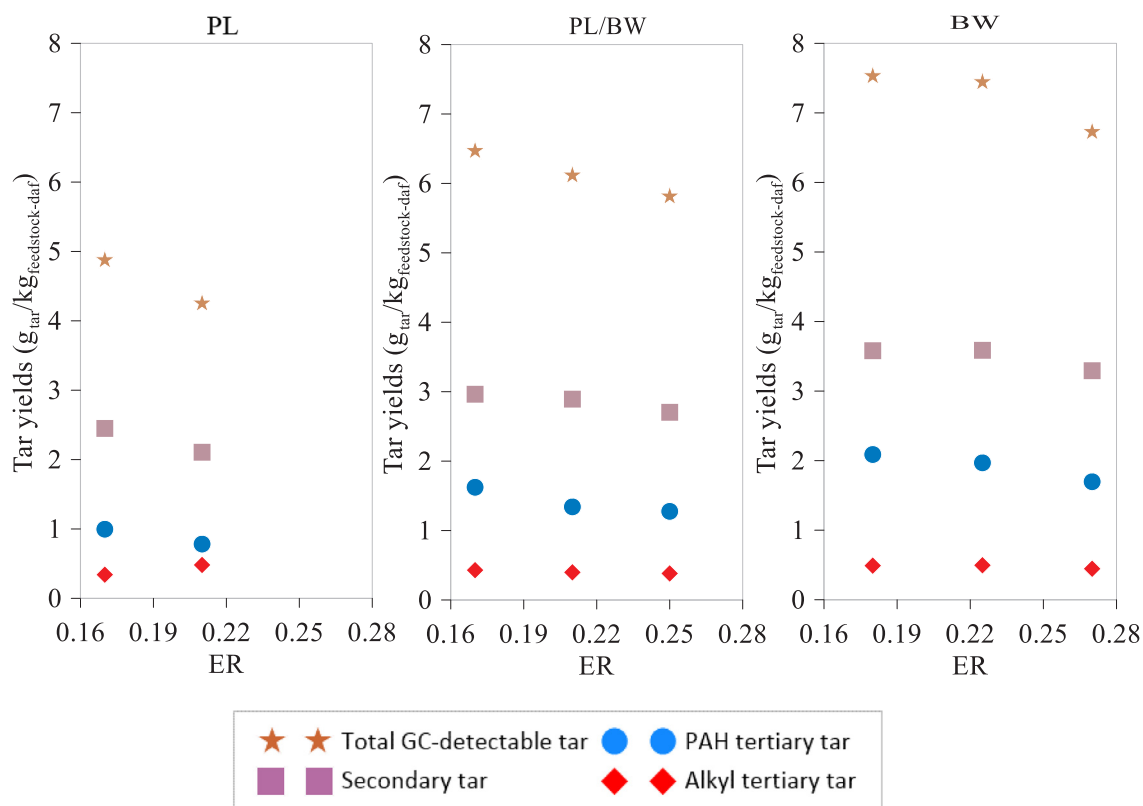


Fig. 5. Tar groups classified according to Milne *et al.*, 1998 and total GC- detectable tar as a function of ER.

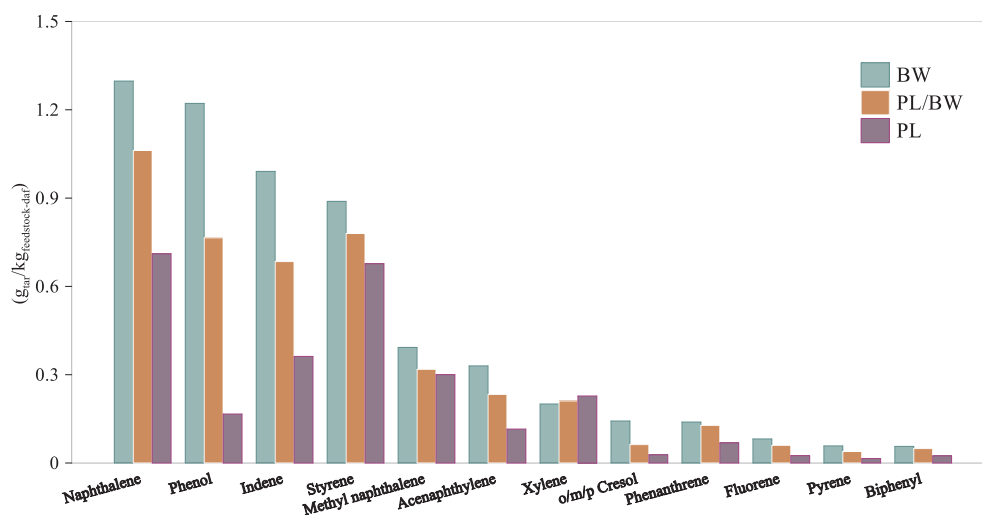


Fig. 6. Yield of individual tar compounds as a function of fuel at the lowest ER.

detectable tar and PAH compared to cellulose and hemicellulose [14,40,41]. Although the chemical content of all tested fuels was not investigated, in the study of Font Palma [14] the chemical analysis of several types of woody biomass (not including beech wood) along with the one of PL are given, showing that the lignin content of all woody biomass is superior to PL. Tar yield of PL/BW falls between the two fuels. Due to the moderate operating temperature of 750 °C, secondary tar is predominant group in all cases, whereas alkyl tertiary tar displays the lowest yields. Generally, it is expected that the yield of PAH tertiary tar would increase at temperatures higher than 750 °C, through decomposition of secondary tar compounds and subsequent recombination into PAH tertiary tar compounds. On the other hand, alkyl tertiary tar develop at temperatures 750–850 °C, acting as intermediates

between secondary and PAH tertiary tar groups, while at temperatures higher than 850 °C, reform into unsubstituted PAHs [42]. However due to the limitation of operating temperature range, it was not possible to study in detail the evolution profiles of PAH and alkyl tertiary tar groups.

The amount of detected but not identified tar is in the range 20–25% for all fuels and was calculated by subtracting the identified tar compounds from total GC-detectable tar. Fig. 6 shows twelve tar compounds present in all fuels and with quantity  $\geq 0.05 \text{ g}_{\text{tar}}/\text{kg}_{\text{feedstock-daf}}$  at the lowest ER (0.17/0.18). The rest of the tar compounds are given in supplementary file (Tables S1–S8). Naphthalene is the most abundant compound in the PAH tertiary tar group followed by phenol, indene and styrene which belong to the secondary tar group. Overall

**Table 6**  
Mass balance for tests with PL/BW and BW fuels.

Elements	PL/BW (ER = 0.17)			PL/BW (ER = 0.21)			PL/BW (ER = 0.25)		
	Input	Output	Relative error (%)	Input	Output	Relative error (%)	Input	Output	Relative error (%)
C (kg/h)	0.228	0.197	13.37	0.228	0.197	13.34	0.228	0.199	12.56
H (kg/h)	0.033	0.030	10.11	0.033	0.031	5.33	0.033	0.043	-28.9
N (kg/h)	0.840	0.868	-3.41	0.810	0.826	-1.25	0.790	0.8	-1.21
Elements	BW (ER = 0.18)			BW (ER = 0.225)			BW (ER = 0.27)		
	Input	Output	Relative error (%)	Input	Output	Relative error (%)	Input	Output	Relative error (%)
C (kg/h)	0.232	0.201	13.39	0.232	0.210	9.55	0.232	0.222	4.56
H (kg/h)	0.036	0.029	20.3	0.036	0.032	10.98	0.036	0.034	6.35
N (kg/h)	0.824	0.832	-0.97	0.800	0.818	-2.22	0.776	0.795	-2.41

Relative error:  $[(\text{Input}-\text{Output})/\text{Input}] * 100\%$ .

naphthalene is considered as very stable compound remaining present at temperatures of 900 °C even after catalytic tar cracking [43,44]. It is formed by either the breakdown of heavy tar (GC-undetectable and heavy PAH), or by polymerisation reactions from smaller building blocks.

### 3.6. Mass balance

Table 6 presents mass balance calculations pertaining to the PL/BW and BW in order to ascertain the accuracy of the experimental measurements. Mass balance for the PL was not performed because the material from the cyclone was not collected for one of the tests at 750 °C. However, the mass balance for the PL experiments conducted at the temperature of 700 °C was reported elsewhere [45]. The input streams comprise of solid feedstock, air, nitrogen and moisture content whilst the output consists of dry gas, unconverted material collected from the bed and cyclone (char and ash), along with the moisture present in the gas. It should be noted that accumulation of char and ash in the bed were estimated as average over the day of the experiments, whereas material from the cyclone was collected at the end of each experimental test. From Table 6, it can be observed that most of the relative errors of the mass balances read below 15% and are considered within the acceptable limits. Furthermore, deviations in hydrogen balance can be attributed to lack of information regarding elements such as ammonia but also due to errors in moisture determination and non-inclusion of heavy hydrocarbon compounds in the tar.

## 4. Conclusions

Gasification of PL, blend of PL with BW and BW alone were studied in a lab-scale bubbling fluidised bed reactor. It was demonstrated that blending PL with BW can prevent agglomeration occurring at 750 °C, but when the temperature is increased at 800 °C, again agglomeration interrupts the smooth operation of the gasifier. ER had a negative effect on LCV, whereas it enhanced CCE. The highest LCV (4.96 MJ/Nm<sup>3</sup>) and CCE (91.6%) were reported while gasifying the BW alone. Tar yields are affected by the fuel type and decreased with ER. As expected due to the higher lignin content compared to the other two fuels, BW showed the highest amount of GC-detectable tar at the lowest tested ER (7.52 gtar/kg<sub>feedstock-daf</sub>). In the cases of PL and PL/BW, significant amounts of nitrogen-containing tar compounds were identified due to higher nitrogen content in PL compared to BW.

## Declaration of Competing Interest

The authors declare that they have no known competing financial interests or personal relationships that could have appeared to influence the work reported in this paper.

## Acknowledgement

The authors would like to express their gratitude and appreciation to the European Commission for the financial support of the experimental campaign through the BRISK2 project (grant agreement number 731101) and to the staff of the Energy Research Centre of the Netherlands (ECN part of TNO) for hosting the experimental campaign. This work is supported by the Engineering and Physical Sciences Research Council (EPSRC, EP/P004636/1, UK). The financial support from EPSRC is gratefully acknowledged. Daya Shankar Pandey acknowledges funding from the Global Challenges Research Fund (GCRF, R5004, UK).

## Appendix A. Supplementary data

Supplementary data to this article can be found online at <https://doi.org/10.1016/j.fuel.2019.116660>.

## References

- [1] Yu H, Zhang Z, Li Z, Chen D. Characteristics of tar formation during cellulose, hemicellulose and lignin gasification. *Fuel* 2014;118:250–6. <https://doi.org/10.1016/j.fuel.2013.10.080>.
- [2] Bioenergy Europe statistical report 2018:1–201. <https://bioenergyeurope.org/statistical-report-2018/> (accessed May 15, 2019).
- [3] Abelha P, Franco C, Pinto F, Lopes H, Gulyurtlu I, Gominho J, et al. Thermal conversion of *Cynara cardunculus* L. and mixtures with *Eucalyptus globulus* by fluidized-bed combustion and gasification. *Energy Fuels* 2013;27:6725–37. <https://doi.org/10.1021/ef401246p>.
- [4] Ong Z, Cheng Y, Maneerung T, Yao Z, Tong YW, Wang CH, et al. Co-gasification of woody biomass and sewage sludge in a fixed-bed downdraft gasifier. *AIChE J* 2015. <https://doi.org/10.1002/aic.14836>.
- [5] You S, Wang W, Dai Y, Tong YW, Wang C-H. Comparison of the co-gasification of sewage sludge and food wastes and cost-benefit analysis of gasification- and incineration-based waste treatment schemes. *Bioresour Technol* 2016;218:595–605. <https://doi.org/10.1016/j.biortech.2016.07.017>.
- [6] Billen P, Costa J, Van Der Aa L, Van Caneghem J, Vandecasteele C. Electricity from poultry manure: A cleaner alternative to direct land application. *J Clean Prod* 2015;96:467–75. <https://doi.org/10.1016/j.jclepro.2014.04.016>.
- [7] Crawford KW. A review of energy production systems through the utilization of poultry litter as a fuel source and determination of feasibility for North Carolina farming operations. 2013.
- [8] Kelleher BP, Leahy JJ, Henihan AM, O'dwyer TF, Sutton D, Leahy MJ. Advances in poultry litter disposal technology-a review. *Bioresour Technol* 2002;83:27–36.
- [9] Dion LM, Lefsrud M, Orsat V, Cimon C. Biomass gasification and syngas combustion for greenhouse CO<sub>2</sub> enrichment. *BioResources* 2013;8:1520–38. <https://doi.org/10.15376/biores.8.2.1520-1538>.
- [10] Gómez-Barea A, Leckner B. Modeling of biomass gasification in fluidized bed. *Prog Energy Combust Sci* 2010;36:444–509. <https://doi.org/10.1016/j.pecc.2009.12.002>.
- [11] Basu P. Biomass gasification and pyrolysis: practical design and theory. Academic press; 2010.
- [12] Milne TA, Evans RJ, Abatzoglou N. Biomass Gasifier tars: Their nature, formation, and conversion. 1998.
- [13] Mayerhofer M, Fendt S, Spliethoff H, Gaderer M. Fluidized bed gasification of biomass – In bed investigation of gas and tar formation. *Fuel* 2014;117:1248–55. <https://doi.org/10.1016/j.fuel.2013.06.025>.

- [14] Font Palma C. Modelling of tar formation and evolution for biomass gasification: a review. *Appl Energy* 2013;111:129–41. <https://doi.org/10.1016/j.apenergy.2013.04.082>.
- [15] Rabou LPLM, Zwart RWR, Vreugdenhil BJ, Bos L. Tar in biomass producer gas, the Energy research Centre of The Netherlands (ECN) experience: an enduring challenge. *Energy Fuels* 2009;23:6189–98. <https://doi.org/10.1021/ef9007032>.
- [16] Huang Y, Anderson M, McIlveen-Wright D, Lyons GA, McRoberts WC, Wang YD, et al. Biochar and renewable energy generation from poultry litter waste: a technical and economic analysis based on computational simulations. *Appl Energy* 2015;160:656–63. <https://doi.org/10.1016/j.apenergy.2015.01.029>.
- [17] Pandey DS, Kwapinska M, Gómez-Barea A, Horvat A, Fryda LE, Rabou LPLM, et al. Poultry litter gasification in a fluidized bed reactor: effects of gasifying agent and limestone addition. *Energy Fuels* 2016;30(4):3085–96. <https://doi.org/10.1021/acs.energyfuels.6b00058>.
- [18] Taupe NC, Lynch D, Wnietzak R, Kwapinska M, Kwapinski W, Leahy JJ. Updraft gasification of poultry litter at farm-scale. A case study. *Waste Manag* 2016;50:324–33. <https://doi.org/10.1016/j.wasman.2016.02.036>.
- [19] Cavalaglio G, Coccia V, Cotana F, Gelosia M, Nicolini A, Petrozzi A. Energy from poultry waste: an Aspen Plus-based approach to the thermo-chemical processes. *Waste Manag* 2018;73:496–503. <https://doi.org/10.1016/j.wasman.2017.05.037>.
- [20] Hussein MS, Burra KG, Amano RS, Gupta AK. Temperature and gasifying media effects on chicken manure pyrolysis and gasification. *Fuel* 2017;202:36–45. <https://doi.org/10.1016/j.fuel.2017.04.017>.
- [21] Cotana F, Coccia V, Petrozzi A, Cavalaglio G, Gelosia M, Merico MC. Energy valorization of poultry manure in a thermal power plant: Experimental campaign. *Energy Procedia* 2014;45:315–22. <https://doi.org/10.1016/j.egypro.2014.01.034>.
- [22] Burra KG, Hussein MS, Amano RS, Gupta AK. Syngas evolutionary behavior during chicken manure pyrolysis and air gasification. *Appl Energy* 2016;181:408–15. <https://doi.org/10.1016/j.apenergy.2016.08.095>.
- [23] Ng WC, You S, Ling R, Gin KYH, Dai Y, Wang CH. Co-gasification of woody biomass and chicken manure: Syngas production, biochar reutilization, and cost-benefit analysis. *Energy* 2017;139:732–42. <https://doi.org/10.1016/j.energy.2017.07.165>.
- [24] Tańczuk M, Junga R, Werle S, Chabiński M, Ziółkowski Ł. Experimental analysis of the fixed bed gasification process of the mixtures of the chicken manure with biomass. *Renew Energy* 2019;136:1055–63. <https://doi.org/10.1016/j.renene.2017.05.074>.
- [25] Rettenmeier – Homepage n.d. <https://www.reettenmeier.com/en.html> (accessed October 15, 2019).
- [26] Wen CY, Yu YH. A Generalized Method for Predicting the Minimum Fluidization Velocity. *AIChE J* 1966;12:610–2.
- [27] Horvat A, Kwapinska M, Xue G, Dooley S, Kwapinski W, Leahy JJ. Detailed measurement uncertainty analysis of solid-phase adsorption-total gas chromatography (GC)-detectable tar from biomass gasification. *Energy Fuels* 2016;30:2187–97. <https://doi.org/10.1021/acs.energyfuels.5b02579>.
- [28] Kwapinska M, Xue G, Horvat A, Rabou LPLM, Dooley S, Kwapinski W, et al. Fluidized Bed Gasification of Torrefied and Raw Grassy Biomass (*Miscanthus × giganteus*). the Effect of Operating Conditions on Process Performance. *Energy Fuels* 2015;29:7290–300. <https://doi.org/10.1021/acs.energyfuels.5b01144>.
- [29] Campoy M, Gómez-Barea A, Ollero P, Nilsson S. Gasification of wastes in a pilot fluidized bed gasifier. *Fuel Process Technol* 2014;121:63–9. <https://doi.org/10.1016/j.fuproc.2013.12.019>.
- [30] Arena U, Di Gregorio F. Energy generation by air gasification of two industrial plastic wastes in a pilot scale fluidized bed reactor. *Energy* 2014;68:735–43. <https://doi.org/10.1016/j.energy.2014.01.084>.
- [31] Dupont C, Boissonnet G, Seiler J-M, Gauthier P, Schweich D. Study about the kinetic processes of biomass steam gasification. *Fuel* 2007;86:32–40. <https://doi.org/10.1016/j.fuel.2006.06.011>.
- [32] Nilsson S, Gómez-Barea A, Fuentes-Cano D, Haro P, Pinna-Hernández G. Gasification of olive tree pruning in fluidized bed: experiments in a laboratory-scale plant and scale-up to industrial operation. *Energy Fuels* 2017;31:542–54. <https://doi.org/10.1021/acs.energyfuels.6b02039>.
- [33] Kim YD, Yang CW, Kim BJ, Kim KS, Lee JW, Moon JH, et al. Air-blown gasification of woody biomass in a bubbling fluidized bed gasifier. *Appl Energy* 2013;112:414–20. <https://doi.org/10.1016/j.apenergy.2013.03.072>.
- [34] Arena U, Di Gregorio F. Gasification of a solid recovered fuel in a pilot scale fluidized bed reactor. *Fuel* 2014;117:528–36. <https://doi.org/10.1016/j.fuel.2013.09.044>.
- [35] Xue G, Kwapinska M, Horvat A, Kwapinski W, Rabou LPLM, Dooley S, et al. Gasification of torrefied *Miscanthus × giganteus* in an air-blown bubbling fluidized bed gasifier. *Bioresour Technol* 2014;159:397–403. <https://doi.org/10.1016/j.biortech.2014.02.094>.
- [36] Arena U. Process and technological aspects of municipal solid waste gasification. A review. *Waste Manag* 2012;32:625–39. <https://doi.org/10.1016/j.wasman.2011.09.025>.
- [37] Chen H, Li B, Yang H, Yang G, Zhang S. Experimental investigation of biomass gasification in a fluidized bed reactor. *Energy Fuels* 2008;22:3493–8. <https://doi.org/10.1021/ef800180e>.
- [38] Horvat A, Kwapinska M, Xue G, Rabou LPLM, Pandey DS, Kwapinski W, et al. Tars from Fluidized Bed Gasification of Raw and Torrefied *Miscanthus × giganteus*. *Energy Fuels* 2016;30:5693–704. <https://doi.org/10.1021/acs.energyfuels.6b00532>.
- [39] Horvat A, Pandey DS, Kwapinska M, Mello BB, Gómez-Barea A, Fryda LE, et al. Tar yield and composition from poultry litter gasification in a fluidised bed reactor: effects of equivalence ratio, temperature and limestone addition. *RSC Adv* 2019;9:13283–96. <https://doi.org/10.1039/c9ra02548k>.
- [40] Amen-Chen C, Pakdel H, Roy C. Production of monomeric phenols by thermochemical conversion of biomass: a review. *Bioresour Technol* 2001;79:277–99. [https://doi.org/10.1016/S0960-8524\(00\)00180-2](https://doi.org/10.1016/S0960-8524(00)00180-2).
- [41] Valderrama Ríos ML, González AM, Lora EES, Almazán del Olmo OA. Reduction of tar generated during biomass gasification: a review. *Biomass Bioenergy* 2018;108:345–70. <https://doi.org/10.1016/j.biombioe.2017.12.002>.
- [42] Van Paasen SVB, Kiel JHA. Tar formation in a fluidised-bed gasifier: Impact of fuel properties and operating conditions. *Kardiol Pol* 2004;67:58. doi: ECN-C-04-013.
- [43] Berruoco C, Montané D, Matas Güell B, Del Alamo G. Effect of temperature and dolomite on tar formation during gasification of torrefied biomass in a pressurized fluidized bed 2014. doi:10.1016/j.energy.2013.12.035.
- [44] Devi L, Ptasinski KJ, Janssen FJJG. Pretreated olivine as tar removal catalyst for biomass gasifiers: investigation using naphthalene as model biomass tar. *Fuel Process Technol* 2005;86:707–30. <https://doi.org/10.1016/j.fuproc.2004.07.001>.
- [45] Katsaros G, Pandey DS, Horvat A, Tassou S. Low temperature gasification of poultry litter in a lab-scale fluidized reactor. *Energy Procedia* 2019;161:57–65. <https://doi.org/10.1016/j.egypro.2019.02.058>.